

# Nanoscale

Accepted Manuscript



This is an *Accepted Manuscript*, which has been through the Royal Society of Chemistry peer review process and has been accepted for publication.

*Accepted Manuscripts* are published online shortly after acceptance, before technical editing, formatting and proof reading. Using this free service, authors can make their results available to the community, in citable form, before we publish the edited article. We will replace this *Accepted Manuscript* with the edited and formatted *Advance Article* as soon as it is available.

You can find more information about *Accepted Manuscripts* in the [Information for Authors](#).

Please note that technical editing may introduce minor changes to the text and/or graphics, which may alter content. The journal's standard [Terms & Conditions](#) and the [Ethical guidelines](#) still apply. In no event shall the Royal Society of Chemistry be held responsible for any errors or omissions in this *Accepted Manuscript* or any consequences arising from the use of any information it contains.

# An Intestinal Trojan Horse for Gene Delivery

Haisheng Peng<sup>1,4</sup>, Chao Wang<sup>2</sup>, Xiaoyang Xu<sup>3</sup>, Chenxu Yu<sup>2</sup>, and Qun Wang<sup>1,\*</sup>

<sup>1</sup>*Department of Chemical and Biological Engineering, <sup>2</sup>Department of Agricultural and Biosystems Engineering, Iowa State University, Ames, IA 50011, United States*

<sup>3</sup>*Department of Chemical, Biological, and Pharmaceutical Engineering, New Jersey Institute of Technology, Newark, NJ 07102, United States*

<sup>4</sup>*Department of Pharmaceutics, Daqing Campus, Harbin Medical University, Daqing, 163319, China*

**\* Corresponding author:**

Qun Wang, Ph. D.

Department of Chemical and Biological Engineering  
Iowa State University  
2114 Sweeney Hall  
Ames, Iowa 50011  
Office: (515) 294-4218  
Fax: (515) 294-8216  
E-mail: qunwang@iastate.edu

**Abstract:** Intestinal epithelium forms an essential element of mucosal barrier and plays a critical role in the pathophysiologic response of different enteric disorders and diseases. As the major enteric dysfunction of the intestinal tract, inflammatory bowel disease is a genetic disease which results from the inappropriate and exaggerated mucosal immune response to normal constituents in the mucosal microbiota environment. Intestine targeted drug delivery system has unique advantages in the treatment of inflammatory bowel disease. As a new conception in drug delivery, the Trojan horse system with the synergy of nanotechnology and host cells can achieve better therapeutic efficacy to specific diseases. Here, we demonstrated the feasibility to encapsulate DNA-functionalized gold nanoparticles into primary isolated intestinal stem cells to form an intestinal Trojan horse for gene regulation therapy of inflammatory bowel disease. This proof-of-concept intestinal Trojan horse will have a wide variety of applications in diagnosis and therapy for the treatment of enteric disorders and diseases.

**Keywords:** Intestinal stem cells; gold nanoparticles; Trojan horse; gene delivery

## 1. Introduction

As the major organ in mammals, the intestine is both a catalytic and absorptive site where most of the chemical digestion, nutrient and drug absorption in the gastrointestinal (GI) tract take place. As the interface of intestinal tract, intestinal epithelium forms an essential element of mucosal barrier and plays a critical role in the pathophysiologic response to different enteric disorders and diseases, such as inflammatory bowel diseases (IBD). IBD define a group of idiopathic inflammatory disorders of the GI tract characterized by chronic and sometimes irreversible impairment of gastrointestinal structure and function<sup>1</sup>. Pathological factors may trigger IBD by breaking the mucosal barrier, stimulating immune responses, and/or altering the balance between beneficial and pathogenic enteric bacteria in genetically susceptible individuals<sup>2</sup>. It is believed that IBD is a genetic disease which results from the inappropriate and exaggerated mucosal immune response to normal constituents in the mucosal microbiota environment.

Drug delivery system targeting to intestine has unique advantages in the treatment of IBD<sup>3,4</sup>. The therapeutic efficacy is dependent on the on-site concentration of the drug at the intestinal mucosa<sup>5</sup>. Thus, it's ideal to deliver drugs targeting to the inflammation sites of IBD patients to minimize the potential systemic adverse effects. Nanoparticles, which can protect and release conjugated drugs on-site, have shown their ability to accumulate in the inflamed intestinal tissues<sup>4,6</sup>. Previous research has demonstrated the promising potential of nanoparticle-based treatments for IBD<sup>7,8</sup>. However, difficulties in optimizing the adhesion and systemic absorption of

nanoparticles have significantly limited their use in treatment of IBD<sup>9</sup>.

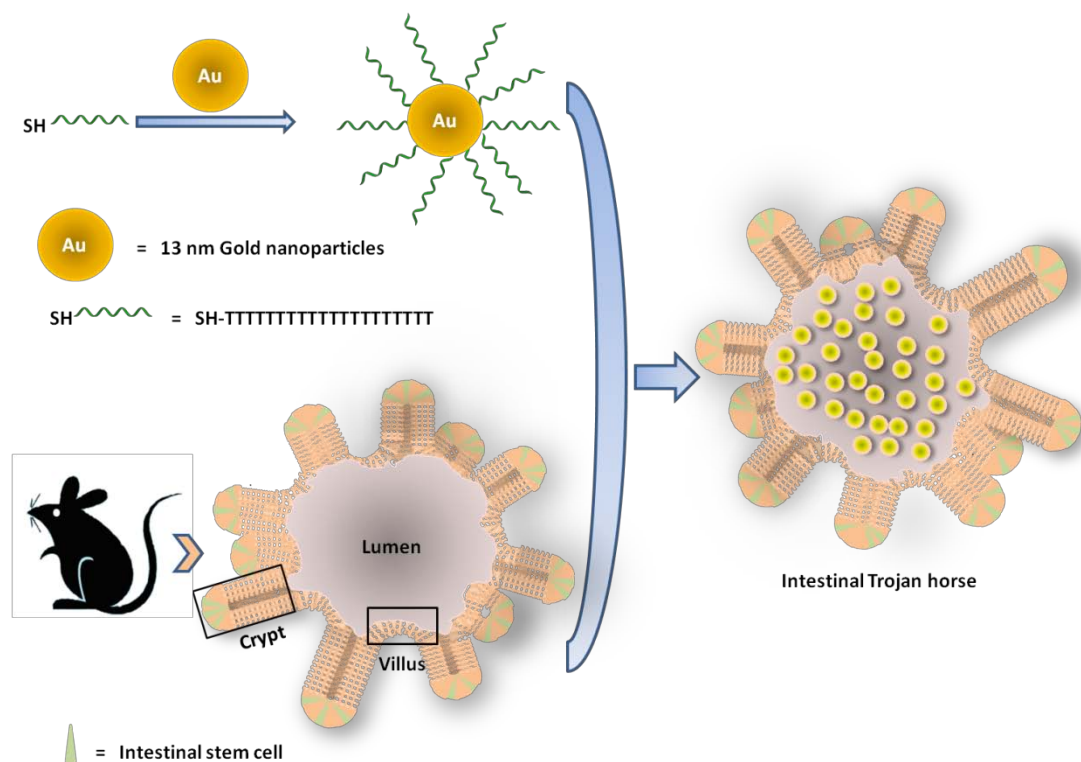
As a new conception in drug delivery, the Trojan horse system with the synergy of nanotechnology and host cells has gotten intense attention in recent years. The therapeutic nanoparticles can be loaded into host cells *ex vivo* due to endocytosis. Then the nanoparticles encapsulated cell, “Trojan horse”, could be injected back into body as delivery vector for therapeutic purpose<sup>10, 11</sup>. The strategy to use Trojan horse system for drug delivery can achieve improved biodistribution, increased local drug concentration, extended retention time, prolonged dosing intervals, and enhanced therapeutic efficacy. Moreover, Trojan horse using donor cells from recipients may have complicated mechanisms to avoid the immune system attack, home to specific tissues, cross impermeable barriers, and modulate their microenvironments. Because of these unique characteristics, Trojan horse is a novel class of therapeutics and drug carriers with high specificity and long persistence. However, one big challenge of this Trojan horse strategy is to ensure the intercellular drug cargos remaining inactive and nontoxic to their host cells until the payload has been delivered to the target tissue.

The DNA-functionalized gold nanoparticles (GNPs) have been extensively used in biomedicine, such as probes in diagnostic system<sup>12</sup>, as well as therapeutic agents for cellular gene regulation<sup>13</sup>. The nontoxic GNPs can act as an antisense agent to scavenge mRNA within the cells efficiently by their cooperative binding properties<sup>14</sup>, which facilitate the endocytosis<sup>15</sup>. The dense packing of DNA of the shell on DNA-functionalized GNPs also facilitates the dispersion of nanoparticles in cell culture medium with high salts and serum concentration. This property of

DNA-functionalized GNPs play a critical role in the inhibition of enzymatic nucleic acid degradation<sup>16</sup>. Furthermore, due to the high presence of positive charged proteins in the inflamed intestines<sup>17</sup>, DNA-functionalized GNPs with a negative surface charge may more easily adhere to denuded mucosa. All these features of DNA-functionalized GNPs make them the excellent candidates to be encapsulated within host cells as Trojan horse for efficient gene regulation therapies for IBD.

Stem cell therapy using live stem cells to treat diseases is a rapidly growing area of translational medicine. Stem cell originated drug delivery systems have been actively explored thanks to their advantages over synthetic drug delivery systems<sup>18-21</sup>. Its success depends on the appropriate control of the fate and function of stem cells. Enhanced survivability, proliferation, and differentiation of donor cells are desirable for therapeutic applications. Due to the recent advancements in the identification of specific adult stem cells, *in vitro* model of intestinal stem cells (ISCs) has been designed<sup>22</sup>. As the cell of origin, single intestinal stem cell can build crypt-villus structure of intestinal epithelium *in vitro*<sup>23</sup>. The self-renewing intestinal organoids could be established by a well-defined set of growth factors with uniform presentation<sup>23</sup>. The isolated ISCs autonomously generate multicellular architecture in a highly stereotypical fashion which is reminiscent of normal intestine. Therefore, ISCs have great potential in the field of intestinal therapeutics. This self-renewed intestinal “organoid” can be used to treat enteric disorders and diseases, such as intestinal infection, radiation injury, and IBD<sup>22, 24</sup>. They are also good candidates as cell hosts to compose intestinal Trojan horse delivery system.

In current study, we isolated primary ISCs from mice and expanded them *ex vivo*. The harvested ISCs dramatically grew into cauliflower-like organoid structures that contained large numbers of separate crypts. These intestinal organoids developed the correct overall multicellular mucosal architecture with both Paneth cells and stem cells contained within the structures. When the ISCs were incubated with DNA-functionalized GNPs, the intestinal organoids encapsulated the nanoparticles within the lumen to form a Trojan horse. This proof-of-concept intestinal Trojan horse demonstrated the feasibility of gene regulation therapies for IBD. We believe that this work will explore the design and manufacture of ISCs originated drug delivery systems. This intestine specific Trojan horse platform will have a wide variety of applications in diagnosis and therapy for the treatment of enteric disorders and diseases. As showed in **Scheme 1**, a rationally designed intestinal “Trojan horse” delivery system using a combination of ISCs and nanoparticles offers a novel and potentially advantageous approach to treat of IBD.



**Scheme 1.** A novel intestinal “Trojan horse” delivery system employs the synergy of intestinal stem cell and gold nanoparticles for gene delivery.

## 2. Materials and Methods

### 2.1. Materials

All materials and solvents were purchased from Life Technologies and used without further purification unless otherwise stated. Matrigel was purchased from Corning Inc. Growth factors EGF, Noggin and R-spondin-1 were purchased from PeproTech Inc. Nanopure™ water (18 MegaOhm: Barnstead International) was used in all experiments and to prepare buffers. The DNA strands were purchased from Integrated DNA Technologies, Inc., and were purified with HPLC prior to use.

### 2.2. Preparation of Gold Nanoparticles

The 13 nm GNPs were synthesized and functionalized with oligonucleotides according to previously reported methods<sup>25, 26</sup>. Briefly, 13 nm diameter GNPs were prepared by the citrate reduction of HAuCl<sub>4</sub>. An aqueous solution of HAuCl<sub>4</sub> (1 mM, 500 mL) was brought to a reflux in a 3-neck round bottom glass flask while stirring, and then 50 mL of a 38.8 mM trisodium citrate solution was added quickly, which resulted in a change in solution color from light yellow to dark red. The solution was refluxed for an additional 15 minutes, cool to room temperature, and subsequently filtered through a 0.45 μm nylon filter (Micron Separations Inc.).

### 2.3. Preparation of DNA-functionalized Gold Nanoparticles

The oligonucleotide used to functionalize the GNPs was thiol labeled DNA (SH-TTT TTT TTT TTT TTT). The oligonucleotide was purified by reverse-phase high-performance liquid chromatography (RP-HPLC). Prior to use, the disulfide functionality on the oligonucleotides was cleaved by addition of DTT to lyophilized DNA and the resultant mixture incubated at room temperature for 1 h (0.1 M DTT, 0.18 M phosphate buffer (PB), pH 8.0). The cleaved oligonucleotides were purified using a NAP-5 column. Freshly cleaved oligonucleotides were added to GNPs (1 OD/1 mL), and the concentrations of PB and sodium dodecyl sulfate (SDS) were brought to 0.01 M and 0.01%, respectively. The salting process was followed by incubation overnight at room temperature. The solution was brought to 0.1 M NaCl, 10 mM phosphate buffer (pH 7) and allowed to stand overnight. To remove excess oligonucleotides, the GNPs were centrifuged and the supernatant was removed,

leaving a pellet of GNPs at the bottom. The particles then were resuspended in buffer (0.1 M NaCl, 10 mM phosphate buffer, 0.01% SDS pH=7.0). This washing process was repeated for three times.

#### 2.4. Isolation of Primary ISCs

The primary ISCs within the intestinal crypts were isolated from the proximal half of mouse small intestine. The intestine specimen which was harvested from the C57BL/6 (B6) mouse was kindly donated by Professor Albert Jergens at College of Veterinary Medicine of Iowa State University. All animal procedures were conducted with the approval of the Iowa State University Institutional Animal Care and Use Committee.

The mouse small intestine was opened longitudinally and then washed with ice-cold PBS until most of luminal contents were cleared. The intestinal tissue were cut into 2-4 mm pieces with scissors and transferred to a 50 ml falcon tube. 30 ml ice-cold PBS was added to the tube and the fragments were gently washed up and down with a 10 ml pipette. After the intestinal tissue fragments were settling down, the supernatant was discarded. This step was repeated 5~10 times until the supernatant was almost clear. 30 ml ice-cold 2 mM EDTA PBS buffer was added to the 50 ml falcon tube and the tube was gently rocked at 4 °C for 30 minutes. After the intestinal fragments were settled down, the supernatant was removed.

Then, 20 ml ice-cold PBS was added to the tube and the fragments were gently washed up and down with a 10 ml pipette. After settling the fragments down, the

supernatants were inspected to see whether they were enriched with villi or crypts by an inverted microscopy. This procedure was repeated several times until most of crypts were released. Then the crypts fractions were passed through a 70  $\mu\text{m}$  cell strainer (Corning Inc.) and collected into a BSA coated 50 ml falcon tube. The villous fractions left on the strainer were discarded. The crypt fractions were centrifuged at 300 g for 5 minutes to get a cell pellet. The pellet was then re-suspended with 10 ml ice-cold Basal culture medium and transferred into a BSA coated 15 ml falcon tube. The tube was centrifuged again at 150 g for 2 minutes to remove single cells. This washing step was repeated 2~3 times until most of single cells were removed. After all the washing steps were completed, the number of the crypts was counted under an inverted microscopy. The harvested primary intestinal crypts were stored in ice-cold Basal culture medium and hold on ice for later use.

### **2.5. Preparation of ISCs Culture Solution**

The Basal culture medium was made by Advanced DMEM/F12 supplemented with 2 mM GlutaMax, 10 mM HEPES, and 100 U/ml Penicillin/ 100  $\mu\text{g/ml}$  Streptomycin. The obtained Basal culture medium was then homogenously mixed with N2 supplement (1X), B27 supplement (1X), 1 mM N-acetylcysteine, 1  $\mu\text{g/ml}$  R-spondin-1, 100 ng/ml Noggin, and 50 ng/ml EGF to form complete ISCs culture medium for future use.

### **2.6. Preparation of Intestinal Trojan Horse**

10,000 isolated intestinal crypts were added to 1 ml Matrigel and re-suspended. 200  $\mu$ l of above cell encapsulated Matrigel was applied in pre-warmed 48-well Falcon plate (Corning Inc.). The gel was applied on the center of the well so that it can form a flat shape. The plate was then transferred to an incubator and allowed to gelation at 37 °C for 30 minutes. Finally, the 500  $\mu$ l complete ISCs culture medium with growth factors was added to each well and the cell encapsulated gels were cultured in the CO<sub>2</sub> incubator at 37°C. After 24 hours, DNA-functionalized GNPs at a DNA strand concentration of 100 nM were added directly to the cell culture medium. After another 24 hours, the culture medium was changed with complete ISCs culture medium and further changed every other day. The ISCs culture without the treatment of DNA-functionalized GNPs was used as control. The images of intestinal organoids in gels were taken by an inverted microscope Nikon Eclipse 2000.

## **2.7. Viability Assessment of Intestinal Trojan horse**

For whole-mount viability assessment, intestinal Trojan horse was released from Matrigel by mechanical force with a p1000 pipette. Then, intestinal Trojan horse was transferred into Eppendorf tubes. For cell viability assessment, organoids were washed in sterile PBS three times and then incubated for 45 minutes at room temperature with 2  $\mu$ M calcein-AM and 4  $\mu$ M EthD-1 added with PBS. After incubation, these constructs were washed again with PBS in preparation for fluorescence microscopy.

### 3. Results and Discussion

#### 3.1. Characterization of DNA-functionalized GNPs

The conjugation of DNA to the gold nanoparticles was characterized via various methods. UV-Vis spectra of GNPs (Lambda 750, Perkin Elmer, Waltham, MA) before/after DNA conjugation were shown in Figure 1A. The red-shift of the plasmonic peak from 519 nm to 536 nm indicated the conjugation of thiolated DNAs onto the GNPs surfaces. TEM image (Jeol 2100, Jeol Ltd., Tokyo, Japan) of the negatively-stained (with 1% uranyl acetate) DNA-GNP complexes was shown in Figure 1B, also indicating the conjugation of thiolated DNAs to the nanoparticles. Figure 1C and Figure 1D showed the un-coated GNPs and the negatively-stained un-coated GNPs, respectively. As we known, the uranyl acetate (UA) could produce high electron density by interaction with lipids/proteins/nucleic acid phosphate groups. Therefore, UA is commonly used as contrast enhancer of organic molecules in electron microscope measurement. The negatively stained TEM image of DNA-GNP (Fig. 1B) revealed that the thickness of the DNA layer around nanoparticles was approximately 1 nm manifested by the UA staining as a bright ring. However, in the negatively-stained un-coated GNPs control TEM image (Fig. 1D), the contrast was weak and the observation of bright ring was obscure. It was considered that no organic materials surrounded the GNPs and therefore, no enough UA was absorbed around GNPs due to the lack of reaction between nucleic acid and UA.

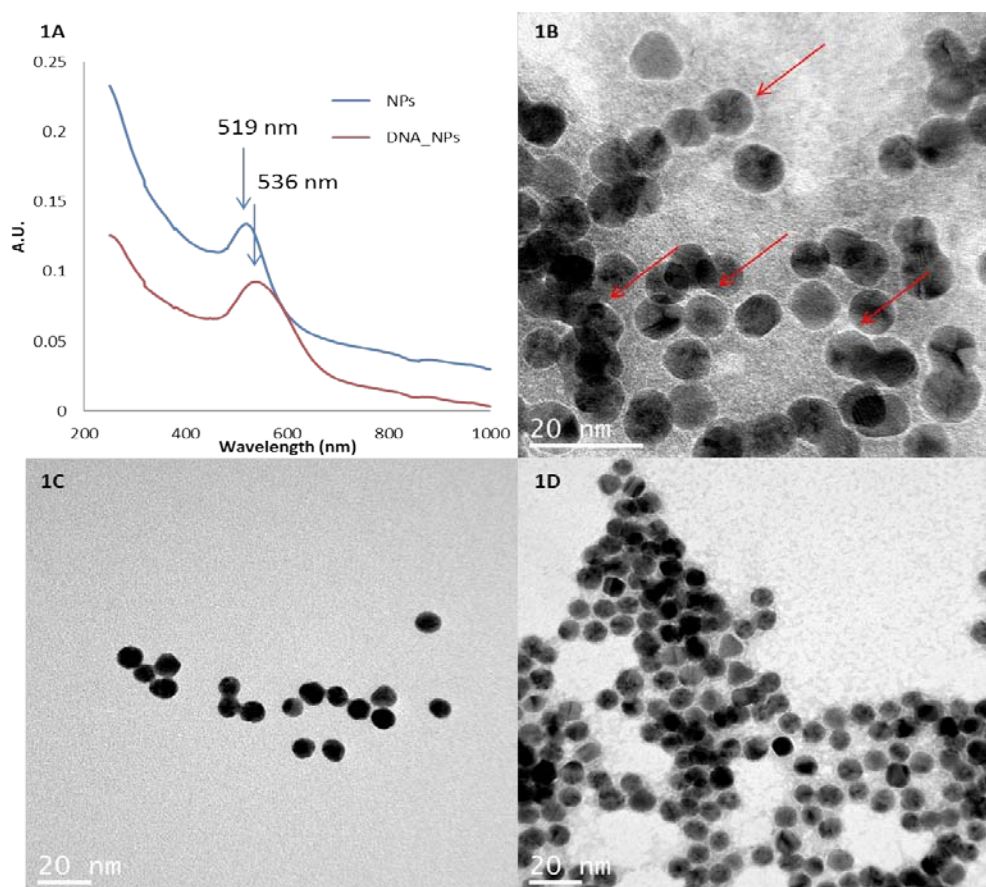


**Figure 1.** Characterization of DNA-GNP conjugation. A, UV-Vis spectra of GNP before/after DNA conjugation, showing red shift of plasmonic peak by 17 nm; B, TEM image of GNP-DNA complexes, arrow pointing to surface-conjugated DNA layers illustrated by negative staining with 1% uranyl acetate; C. TEM image of naked GNP; D. TEM image of GNP control illustrated by negative staining with 1% uranyl acetate.

The zeta potential of the GNPs before/after DNA conjugation was measured (Malvern Nano ZS Zetasizer), and the results were shown in Table 1. The changes in zeta potential at the gold nanoparticle surfaces suggested that the net charges on the particles were changed due to the conjugation of DNAs, which was consistent with the negative charges associated with the DNA backbones. The mobility and conductivity of DNA-GNPs were higher than that of un-coated GNPs. This further confirmed the conjugation of negatively charged DNAs on the GNPs.

Particles	Zeta Potential (mV)	Mob ( $\mu\text{mcm/Vs}$ )	Cond (mS/cm)
GNP	-16.5	-1.29	0.0836
0.01%SDS	-7.0	-0.549	0.173
GNP-control (0.01% SDS)	-4.33	-0.339	0.0735
GNP-DNA (0.01%SDS)	-26.6	-2.089	0.248

**Table 1.** Zeta potential measurement showing addition of negative charges to GNP surfaces due to DNA-conjugation.

### 3.2. Growth of Primary ISCs *ex vivo*

As the control, the isolated primary ISCs were cultured in Matrigel without the treatment of GNPs for 7 days. The *ex vivo* culture system was stable and supported the proliferation and differentiation of ISCs. They expanded and formed organoid structures in which the epithelial cells formed a monolayer at the organoid-gel interface and the extruded cells comprised the lumen. Figure 2 showed the change of morphology of ISCs cultured in Matrigel during 7 days. The isolated primary ISCs got signals from the growth factors in culture medium and constructed a self-organizing and continuously expanding epithelial organoid structure reminiscent of normal intestine. These intestinal organoids autonomously generated asymmetry in a highly stereotypical fashion which led to the rapid formation of crypt-like structures. These crypt-like structures fed into luminal domains where apoptotic cells pinched off into the lumen to constitute the renewing process. These self-renewing intestinal organoids were perfect candidates as cell hosts to compose intestinal Trojan horse for drug delivery.

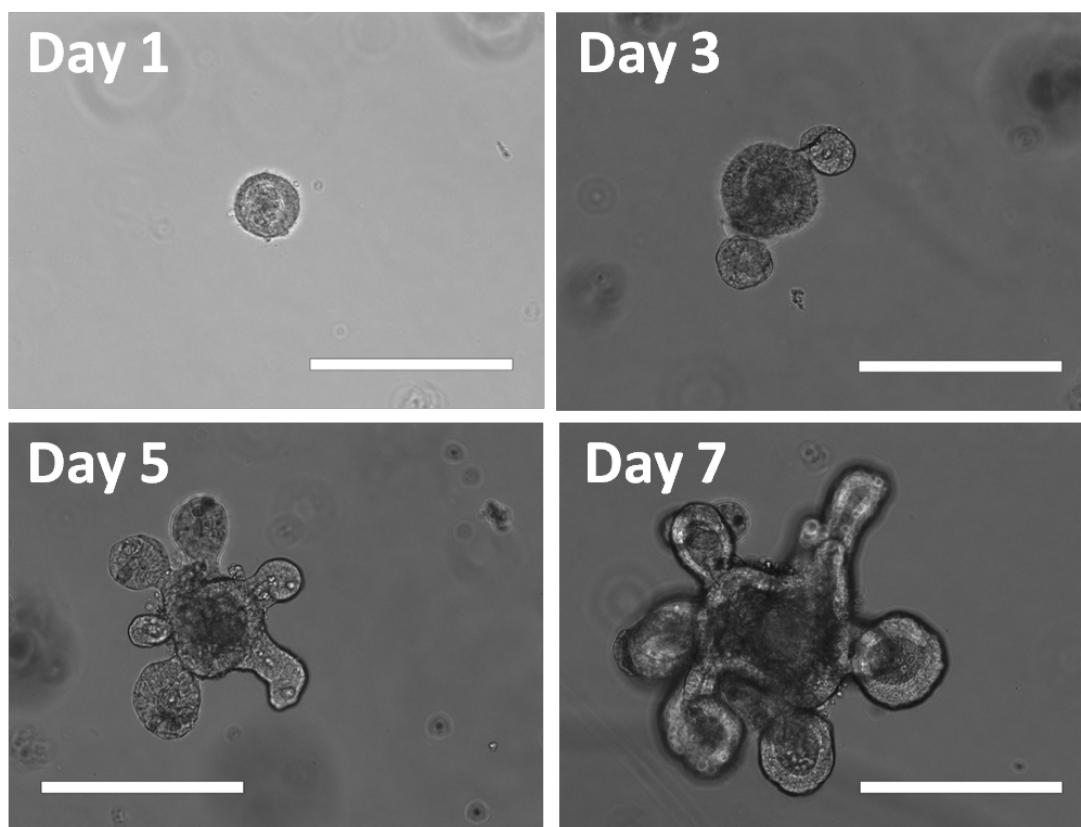


**Figure 2.** The morphology of intestinal stem cells cultured in Matrigel during 7 days. The scale bars were 200  $\mu\text{m}$ .

### 3.3. Growth of Intestinal Trojan horse *ex vivo*

For a Trojan horse system, the cell internalization and sustained retention of nanoparticles in the host cell plays critical roles in determining the therapeutic effects. Because that DNA-functionalized GNPs can effectively enter cells without the use of transfection reagents<sup>27</sup>, we chose DNA-functionalized GNPs as the delivery vehicle to produce the intestinal Trojan horse.

*In vitro*, the color of DNA-functionalized GNPs was in dark red due to the plasmon resonance of the nanoparticles around 520 nm. The encapsulation capability of ISCs to DNA-functionalized GNPs was investigated by an inverted microscope

Nikon Eclipse 2000. As shown in Figure 3, the nanoparticles were successfully internalized by the intestinal organoids. The DNA-functionalized GNPs in the culture medium penetrated the intestinal crypts and epithelium, and then accumulated in the intestinal lumen. The GNPs sustained in the intestinal lumen up to 7 days and put negligible effect on the growth of the intestinal organoids, comparing to the cell culture without the treatment of GNPs.

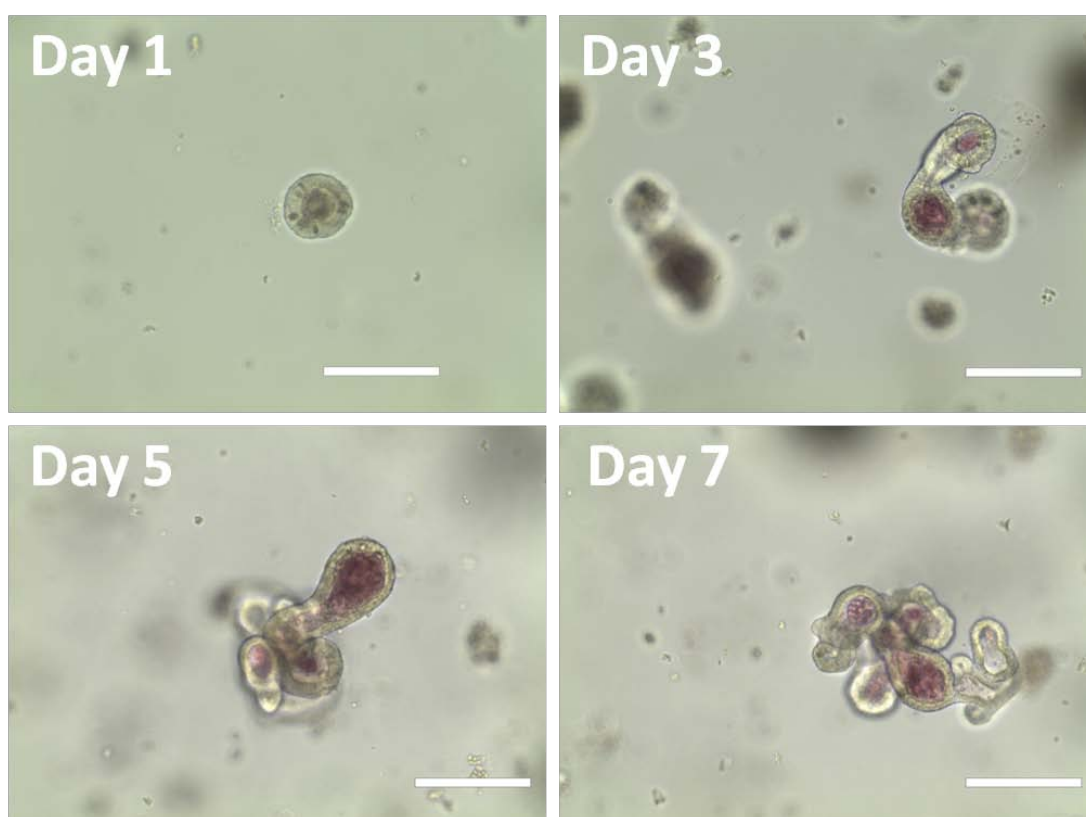


**Figure 3.** The morphology of intestinal Trojan horse cultured in Matrigel during 7 days. The scale bars were 200 μm.

To further test the feasibility of DNA-functionalized GNPs as a carrier for production of intestinal Trojan horse, the whole-mount viability assessment of intestinal Trojan horse was performed. Figure 4 A-D showed that the intestinal

organoids loaded with DNA-functionalized GNPs were viable and robust over the 7 days period. The encapsulated nanoparticles generated little cytotoxic profile within the intestinal organoids even after 7 days of incubation. Moreover, the nanoparticles mediated cell delivery system may overcome the cellular cross resistance of a bunch of therapeutic agents. These pilot results indicated the feasibility of DNA-functionalized GNPs as a gene carrier for intestinal Trojan horse for the therapy of IBD patients.

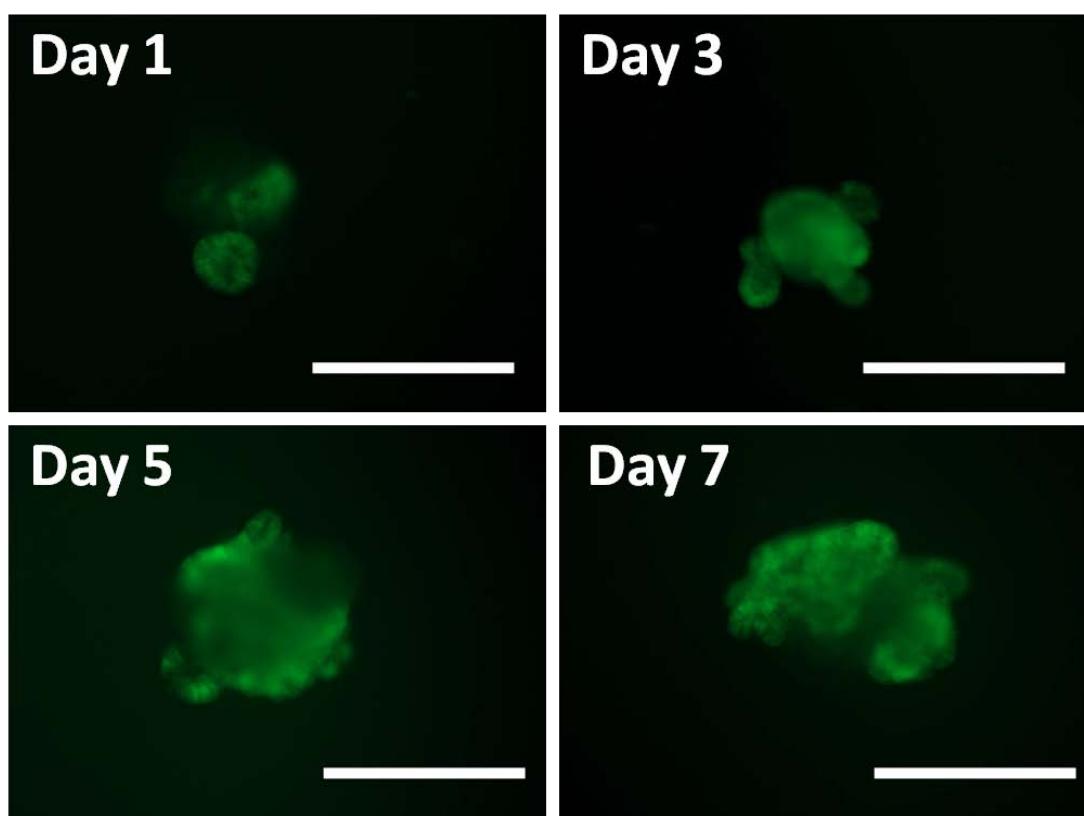


**Figure 4.** The LIVE/DEAD images of intestinal Trojan horse cultured in Matrigel during 7 days. The scale bars were 200  $\mu\text{m}$ .

#### 4. Conclusions

The application of nanotechnology in treating gastrointestinal diseases remains challenging due to the harsh physiological environment in the GI tract. The majority

of the current intestinal targeting nanocarriers have limited stability and therefore with unsatisfactory efficacy. The Trojan horse system with the synergy of nanotechnology and host cells can achieve better therapeutic efficacy to specific diseases.

In this proof-of-conception study, a novel intestinal Trojan horse was developed for gene delivery. We demonstrated the feasibility to encapsulate DNA-functionalized GNPs into primary isolated intestinal stem cells to form a Trojan horse for gene regulation therapies of IBD. In future experiments, GNPs with different surface chemistry at different sizes will be synthesized and used to make the intestinal Trojan horse. The effect of surface coating and particle size on encapsulation efficiency and retention time will be investigated. Although we focused on the gene delivery, the intestinal Trojan horse delivery system could be extended to carry other cargos, such as peptides, growth factors, plasmids, siRNAs, small chemicals, image agents, and even metallic and atomic substances. This intestinal Trojan horse will have a wide variety of applications in diagnosis and therapy for the enteric disorders and diseases.

## **Acknowledgments**

This study was supported by Iowa State University (ISU) President's Initiative on Interdisciplinary Research (PIIR) program, Cyclone Research Partnership Grant and McGee-Wagner Interdisciplinary Research Foundation.

## Reference

1. D. K. Podolsky, *New England Journal of Medicine*, 1991, 325, 928-937.
2. R. B. Sartor, *Nature clinical practice Gastroenterology & hepatology*, 2006, 3, 390-407.
3. D. R. Friend, *Advanced drug delivery reviews*, 2005, 57, 247-265.
4. A. Lamprecht, N. Ubrich, H. Yamamoto, U. Schäfer, H. Takeuchi, P. Maincent, Y. Kawashima and C.-M. Lehr, *Journal of Pharmacology and Experimental Therapeutics*, 2001, 299, 775-781.
5. U. Klotz and M. Schwab, *Advanced drug delivery reviews*, 2005, 57, 267-279.
6. Y. Meissner, Y. Pellequer and A. Lamprecht, *International journal of pharmaceuticals*, 2006, 316, 138-143.
7. A. Lamprecht, H. Yamamoto, H. Takeuchi and Y. Kawashima, *Journal of Pharmacology and Experimental Therapeutics*, 2005, 315, 196-202.
8. B. Moulari, D. Pertuit, Y. Pellequer and A. Lamprecht, *Biomaterials*, 2008, 29, 4554-4560.
9. A. Lamprecht, *Nature Reviews Gastroenterology and Hepatology*, 2010, 7, 311-312.
10. M.-R. Choi, K. J. Stanton-Maxey, J. K. Stanley, C. S. Levin, R. Bardhan, D. Akin, S. Badve, J. Sturgis, J. P. Robinson and R. Bashir, *Nano letters*, 2007, 7, 3759-3765.
11. C.-H. Wu, C. Cao, J. H. Kim, C.-H. Hsu, H. J. Wanebo, W. D. Bowen, J. Xu and J. Marshall, *Nano letters*, 2012, 12, 5475-5480.
12. N. L. Rosi and C. A. Mirkin, *Chemical reviews*, 2005, 105, 1547-1562.
13. N. L. Rosi, D. A. Giljohann, C. S. Thaxton, A. K. Lytton-Jean, M. S. Han and C. A. Mirkin, *Science*, 2006, 312, 1027-1030.
14. A. K. Lytton-Jean and C. A. Mirkin, *Journal of the American Chemical Society*, 2005, 127, 12754-12755.
15. D. A. Giljohann, D. S. Seferos, P. C. Patel, J. E. Millstone, N. L. Rosi and C. A. Mirkin, *Nano letters*, 2007, 7, 3818-3821.
16. D. S. Seferos, A. E. Prigodich, D. A. Giljohann, P. C. Patel and C. A. Mirkin, *Nano letters*, 2008, 9, 308-311.
17. A. Dahan, G. L. Amidon and E. M. Zimmermann, *Expert review of clinical immunology*, 2010, 6, 543-550.
18. C. D. Porada and G. Almeida-Porada, *Advanced drug delivery reviews*, 2010, 62, 1156-1166.
19. A. U. Ahmed, N. G. Alexiades and M. S. Lesniak, *Current opinion in molecular therapeutics*, 2010, 12, 546.
20. F.-J. Müller, E. Y. Snyder and J. F. Loring, *Nature Reviews Neuroscience*, 2006, 7, 75-84.
21. C. Tang, P. J. Russell, R. Martiniello - Wilks, J. Rasko, E. John and A. Khatri, *Stem Cells*, 2010, 28, 1686-1702.
22. D. H. Scoville, T. Sato, X. C. He and L. Li, *Gastroenterology*, 2008, 134, 849-864.
23. T. Sato, R. G. Vries, H. J. Snippert, M. van de Wetering, N. Barker, D. E. Stange, J. H. van Es, A. Abo, P. Kujala and P. J. Peters, *Nature*, 2009, 459, 262-265.
24. A. S. Gulati, S. A. Ochsner and S. J. Henning, *American Journal of Physiology-Gastrointestinal and Liver Physiology*, 2008, 294, G286-G294.
25. J. J. Storhoff, R. Elghanian, R. C. Mucic, C. A. Mirkin and R. L. Letsinger, *Journal of the American Chemical Society*, 1998, 120, 1959-1964.
26. S. J. Hurst, A. K. Lytton-Jean and C. A. Mirkin, *Analytical chemistry*, 2006, 78, 8313-8318.
27. D. A. Giljohann, D. S. Seferos, W. L. Daniel, M. D. Massich, P. C. Patel and C. A. Mirkin,

*Angewandte Chemie International Edition*, 2010, 49, 3280-3294.